Numerical Modeling of Portland Cement Hydration Based on Particle Kinetic Model and Multi-component Concept

I. Maruyama[1], T. Matsushita[2], T. Noguchi[2]

[1]Nagoya University, Nagoya, Japan;
[2]The University of Tokyo, Tokyo, Japan

Abstract
A Numerical hydration model is presented, in which hydration and micro-structural development in Portland cement-based materials can be simulated. In the proposed model, kinetic of mineral component in cement is modeled according to experimental data by XRD-Rietveld analysis, and specific heat of hydration product and unhydrated cement is taken into account to precisely for simulating adiabatic temperature rise of concrete.

1.Introduction

Over the past few decades a number of studies have been made with respect to the modeling of cement hydration [1-3]. In those recent studies, the simulation of intricate and compound processes of cement hydration, especially those focused on micro-mechanics, have utilized the potential of modern computers [4,5]. Two points seem to be helpful in attempting to sketch out what makes it complex to simulate the process of cement hydration and why it needs to be understood using a computer. One is physical aspect. Cement paste matrix, which is composed of cement particles and water is determined by both particle size distribution [1,3] and water-to-cement ratio [7]. In the cement hydration process, cement particles are interconnected and make the structure of the cement paste matrix. This physical aspect affects the rate of cement hydration through the diffusion of ions [3,5]. The second is chemical aspect. Cement is a poly-mineral material and components react with each other, additionally temperature and humid environment have a great influence on the rate of hydration [2,6]. These two aspects have a mutually dependent relationship through diffusion of ions, water, and material formation. This relationship cannot be solved with a simple equation. In this contribution, based on the Tomosawa's model [8], model for hydration process in cement paste matrix named 'CCBM' [Computational Cement Based Material Model] is proposed and its potential for portraying the concrete properties is discussed with experimental results.

2. Hydration model

2.1 Background

Proposed hydration model is based on the fundamental kinetic model for Portland cement developed by Tomosawa [8]. Tomoswa's model, which is

originally given in literature [2], is expressed as a single equation (Eq.(1)) composed of four rate determining coefficients which determine the rate of formation and destruction of initial impermeable layer, the activated chemical reaction process and the following relent diffusion controlled process:

$$-\frac{dr_t}{dt} = \frac{\rho_w C_w}{\gamma_g \rho_c r_t^2} \cdot \frac{1}{\frac{1}{k_d r_t^2} + \frac{1/r_t - 1/R_t}{D_e}^2 + \frac{1}{k_r r_t}} \qquad \text{Eq.(1)}$$

where, r_t is the radius of an unhydrated cement particle (mm), R_t is the total radius of cement particle including the gel layer (mm), D_e is the effective diffusion coefficient of water in the cement gel (mm^2/h), k_r is the coefficient of reaction rate per unit area at reaction front (mm/h), k_d is the coefficient of resistance by protective layer at dormant period (mm/h), g_g is the stoichiometric ratio by mass of water to cement, r_c is density of cement, r_w is density of water, C_w is volumetric density of water in cement paste matrix.

This preliminary approach shows high potential of simulating of hydration process. Four coefficients, however, are just fit parameter in Tomosawa's model and they are not predictable from any information of cement properties. This can be deduced by a fact that the target of modeling of this model is particle hydration process, and not cement paste matrix.

2.2 Assumptions

For the proposed model CCBM, the following assumptions which is originally adopted to Tomosawa's model and additional changes are adopted:

1. The cement particle initiates hydration from the moment that it is brought into contact with water.
2. The hydrate formed by hydration adheres to the cement particle. And hydrate will be covering it up spherically until interparticle contact comes up. And unhydrated cement keeps spherical shape as well. The new hydrate is formed at the surface with no restriction of interparticle contacts. If the surface contacts with the surface of another particle, new hydrate is no longer produced on it.
3. The hydrate has a v times as much as the original cement in volume.
4. The liquid phase, which is assumed to be water, diffuses through the hydrate layer and reaches the surface of the cement particle (reacting front) and chemically reacts with cement. This process continues through hydration process. And part of the hydrate produced at the reacting surface moves out through the layer of hydrate. Hence, equi-molar counter diffusion of water and hydrate (presumably ions) is assumed to be taking place in the hydrate layer.
5. The diffusion coefficient of hydrate layer for water is not different between outer products and inner products. This diffusion coefficient is

affected by tortuosity of gel pore as well as the radius of gel pore in hydrate. This phenomenon can be expressed as a function of degree of hydration.

6. The particle size distribution of cement can be approximated by Rosin-Rammler function. And each particle with the same diameter has the same rate of hydration.
7. Dormant period in the initial process of hydration is assumed that there is a process in which the reaction resistance increases with the increase of degree of hydration in each particle (film formation) followed by a period in which the reaction resistance decreases with increasing thickness of inner products.

2.2 Particle size distribution

Cement particle size distribution will make a large difference in the cement hydration process [9]. When defining the degree of hydration as a ratio of reacted cement volume to initial cement volume, each particle shows a different degree of hydration according to its size. Also, the degree of hydration of total cement paste should account for the different degree of hydration of each particle. In the proposed model. it is assumed that the cement particle distribution can be expressed with the Rosin-Ramler Function (Eq.(2)).

$$V(r_0) = 1 - \exp\left(-b \cdot (2r_0)^n\right) \qquad \text{Eq.(2)}$$

where $V(r_0)$ is the mass ratio of cement particles smaller than particle with radius r_0 (g/g) and b and n are coefficients for distribution.

2.3 Interparticle contact effect

On the other hand, cement particles develop interparticle contacts as hydration proceeds. After formation of interparticle contact, cement hydration is inhibited by the decrease in area for precipitation of hydrate. It follows from this that the water-to-cement ratio of cement paste is significant for determining the process of cement hydration through geometrical features. In the model proposed here, the cement particles with the radius larger than 1 micro are assumed to be arranged in the cement paste matrix homogeneously as a pseudo-6-neighborhood. The word “pseudo-” is used here in the sense that there exists a particle size distribution and it is possible that neighboring particles are not the same size. Additionally the particles with the radius less than 1 micro are usually reacts quite rapid and this reaction should not be affected by the reaction of the other particle geometrically. The interparticle contact effect on the rate of hydration of each particle is modeled as the expanding sphere in the unit cubic cell which is determined by the initial water-to-cement ratio. The size of unit cubic cell is defined by Eq.(3).

$$l = \left(4\pi\left(\omega\rho_c / \rho_w + 1\right)/3\right)^{1/3} \cdot r_0 \qquad \text{Eq.(3)}$$

where l is the length of edge of unit cell corresponding to the cement particle with radius r_0, w is water -to-cement ratio.

The schematic interparticle contact model and the relationship between normalized radius of expanding cement particle (R_t / l) and its free surface is illustrated in Fig. 1.

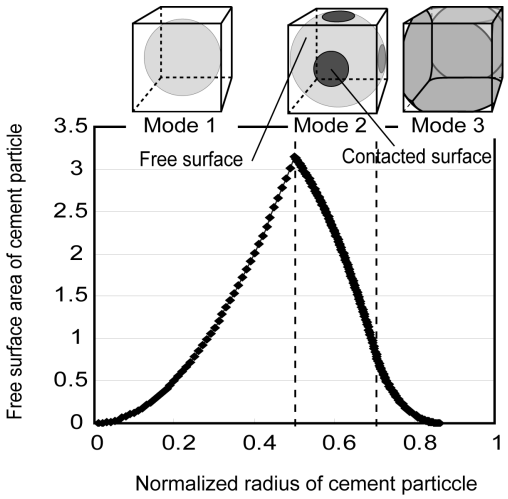

Fig. 1 Schematic of interparticle contact model and free surface area of expanding cement particle as a function of normalized cement radius.

The effect of space limitation on the rate of hydration of cement particle is adopted to Tomosawa's model as Eq.(4) and Eq.(5):

$$-\frac{dr_t}{dt} = \frac{\rho_w C_{st} C_w}{(\gamma_g + \gamma_w)\rho_c r_t^2} \cdot \frac{1}{\frac{1}{k_d r_t^2} + \frac{1/r_t - 1/R_t}{D_e}^2 + \frac{1}{k_r r_t}} \qquad \text{Eq.(4)}$$

$$\frac{dR_t}{dt} = \frac{(\nu - 1) r_t^2}{S(R_t)} \cdot \frac{dr_t}{dt} \qquad \text{Eq.(5)}$$

where R_t is the radius of cement particle with hydrate, γ_w (=0.13) is the ratio of water adsorbed in gel pore to reacted cement (this is not considered in Tomosawa's model), $S(R_t)$ is the function of free surface area on outer products , C_{st} is the coefficient for the effect of interparticle contact defined as $S(R_t)/(4\pi R_t^2)$, ν is assumed to be 2.0, and C_w represents the free energy of water in the paste matrix and is a function of relative humidity, namely $C_w=((rh-0.55)/0.45)^3$, deduced from experiment by Ono [10].

2.4 Pore structure

Free energy of the adsorbed water in gel pore is affected by the environment such as temperature and relative humidity. And this free energy of the adsorbed water govern the rate of hydration process. Therefore water behavior in cement paste matrix represented by pore size

distribution is necessary for modeling the hydration process. In modeling the pore size distribution, a simplified approach of the HYMOSTRUC [5], based on mercury intrusion, is used in this proposed model. The shape of the pore is assumed cylindrical, and the cumulative pore size distribution for the capillary pore can be described mathematically by the following Eq.(6):

$$V_{\le f} = a \ln (f / f_0) \qquad \text{Eq.(6)}$$

where $V_{\le f}$ is the capillary pore volume of all pores with diameter less than f, f is diameter of the capillary pore, f_0 is a minimum capillary pore diameter (2nm), and a is a pore structure constant determined by $a=V_{pore}/\ln(f_{max}/f_0)$. V_{pore} is the total capillary pore volume and, f_{max} is the maximum capillary pore.

Regarding properties of water such as density, vapor pressure, surface tension and so on have been already modeled by several researchers [11] and their model and following isothermal model [12] is adopted for behavior of water in capillary pore.

$$l_w = h_0 \left(\ln(E_{ab}/(RT)) - \ln(-\ln(h))\right) \qquad \text{Eq.(7)}$$

where l_w is thickness of adsorbed water (nm), h_0 is coefficient (0.194nm), E_{ab} is an activation energy of adsorption (18kJ/mol), R is gas constant, and T is temperature(K).

Given the pore size distribution, amount of capillary water and temperature, Kelvin equation can lead the relative humidity in the pore with Eq. (7), and surface tension and density of water.

2.5 Multi-component concept

Clinker minerals, such as alite(C_3S), belite(C_2S), alminate phase(C_3A), and ferrite phase(C_4AF) have their own reactions with water. Hence the composition of cement significantly affect on the rate of hydration. Reactions of the individual cement constituents adopted in the proposed model are summarized in Table 1 and density of cement constituents and hydrates are listed in Table 2.

Assuming that nominal reaction rate per unit area of unhhydrate cement k_r can be given by summation of the each reaction rate of cement constituents $k_{r,i}$, Eq. (14) holds:

$$k_r = \sum a_i \cdot k_{r,i} \qquad \text{Eq.(14)}$$

where a_i is fraction of surface area of each constituents assumed to be equal to volumetric ratio of remained each constituents in unhydrated cement core, and i represents C_3S, C_2S, C_3A, and C_4AF.

Consequently, r_c and g_g are differed during hydration process and are calculated by Eqs. (15) and (16):

$$\rho_c = \sum a_i \rho_i k_{r,i} / \sum a_i k_{r,i} \qquad \text{Eq.(15)}$$

$$\gamma_g = \sum a_i \gamma_i k_{r,i} / \sum a_i k_{r,i} \qquad \text{Eq.(16)}$$

where r_i is density of each mineral component and g_i is stoichiometric ratio by mass of water to each constituents determined by the data in Table 1 and Table 2.

Table 1 Hydration reactions of cement constituents and its heat generation.

	Equation	Heat of hydration (J/g)	
C_3S	$C_3S+2.65H \rightarrow C_{1.7}SH_{1.35} + 1.3CH$	519.0	Eq.(8)
C_2S	$C_3S+1.65H \rightarrow C_{1.7}SH_{1.35} + 0.3CH$	260.0	Eq.(9)
C_3A	$C_3A+3C\bar{S}H_2+26H \rightarrow C_3A\cdot 3C\bar{S}\cdot H_{32}$	1453.0	Eq.(10)
	$2\,C_3A+C_3A\cdot C\bar{S}\cdot H_{12}+4H \rightarrow 3C_3A\cdot C\bar{S}\cdot H_{12}$	996.3	Eq.(11)
C_4AF	$C_4AF+3C\bar{S}H_2+27H \rightarrow C_3AF\cdot 3C\bar{S}\cdot H_{32}+CH$	419.0	Eq.(12)
	$2\,C_4AF+C_3AF\cdot 3C\bar{S}\cdot H_{32}+6H \rightarrow 3\,C_3AF\cdot C\bar{S}\cdot H_{12}+2CH$	276.0	Eq.(13)

Table 2 Density of chemical components concerning cement hydration system.

Component	Density (g/cm^3)	Component	Density (g/cm^3)
C_3S	3.15	$C_{1.7}SH_{1.35}$ *2	2.60
C_2S	3.26	CH	2.24
C_3A	3.04	$C_3A\cdot 3C\bar{S}\cdot H_{32}$	1.73
C_4AF	3.77	$C_3A\cdot C\bar{S}\cdot H_{12}$	1.99
$C\bar{S}H_2$	2.32	$C_3AF\cdot 3C\bar{S}\cdot H_{32}$	1.77
$C_{1.7}SH_4$ *1	2.12	$C_3AF\cdot C\bar{S}\cdot H_{12}$	2.08

*1 :including physically bound water, *2:excluding physically bound water

2.6 Dormant period

As the mechanism of dormant period of hydration process has not been cleared, the rate determining coefficient k_d is phenomenologically determined as follows:

$$k_d = B/\alpha^{1.5} + C\left(r_0 - r_t\right)^{4.0} \qquad \text{Eq.(17)}$$

where B and C is rate determining coefficients and a is averaged degree of hydration of cement.

Eq.(17) reflects experimental results that the dormant period is not affected by the cement particle size and the second peak in calorimeter

test is affected by the cement particle size [13].

2.7 Effect of temperature

The temperature effect on the rate determining coefficients in Eqs.(4) and (17) is modeled with Arrhenyou's low as follows:

$$B = B_{20} \cdot \exp\left(-\beta_1(1/T - 1/293)\right) \quad \text{Eq.(18)}$$

$$D_e = C_{\alpha,T} \cdot D_{e,20} \cdot \exp\left(-\beta_2(1/T - 1/293)\right) \quad \text{Eq.(19)}$$

$$k_{r,i} = k_{r20,i} \cdot \exp\left(-E_i / R(1/T - 1/293)\right) \quad \text{Eq.(20)}$$

where B_{20}, $D_{e,20}$, and $k_{r20,i}$ are value of B, D_e, and $k_{r,i}$ at 293K respectively and b_1, b_2, and E_i are coefficients for temperature dependent of B, D_e, and $k_{r,i}$ respectively. $C_{a,T}$ is a coefficient for taking account of the effect of degree of hydration and curing temperature on $D_{e,20}$.

2.8 Structural change of hydrates

Kondo [1] pointed to the effect of the degree of hydration on the hydrate composition, that is C/S ratio increases with increasing degree of hydration. And several papers reported on an effect of the temperature on the composition of the reaction products [14] and C/S ratio is increased when the curing temperature is elevated [15]. These phenomena partially supported the validity that the effective diffusion coefficient of water in the cement gel D_e is decreased with the increase of degree of hydration and the higher temperature curing, while Tomosawa originally modeled the tendency of decrease in effective diffusion coefficient as a function of degree of hydration [3]. The proposed model CCBM also take into account of these tendencies with phenomenal Eq.(21):

$$C_{\alpha,T} = (1-\alpha)^2 \cdot \left(\frac{0.95}{1+\exp\left((T-333)/2\right)} + 0.05 \right) \quad \text{Eq.(21)}$$

3. Determination of model parameters

In the foregoing chapters some characteristic model features and the relative influence of several rate determining factors of CCBM were discussed qualitatively. This chapter deals with the quantification of the model parameters of Eqs.(4,5,6,14,17,18,19, and 20).

For determination of model parameters, degree of hydration of cement paste was determined with Rietveld analysis whose accuracy is disscussed in ref. [16]. In the experiment, 2 type of cements (NC and LC) with w/c ratio of 0.35 and 0.5 as well as curing condition at 283, 293, and 313 (K) are tested. The chemical composition of cements, mineral composition and coefficients for Rosin-Ramler function determined by the particle distribution test with X-ray scattering are summarized in Table 3

and Table 4.

Samples were prepared as follows: Mix the materials at the specified temperature and seal-cure until the specified age. Cut the specimen to an appropriate size with a diamond cutter and finely pulverize with acetone using a disk mill. After separating the powder from acetone by suction filtration, dry the sample for approximately two weeks in an environment of 15%RH, to obtain a hydration analysis sample. The powder X-ray diffraction was measured under the following conditions: The X-ray source: Cu-Ka; tube voltage: 50 kV; tube current: 250 mA; scan field: 2 (theta) = 5 to 65 deg; step interval: 0.02 deg; and scan speed: 2 deg/min. The TOPAS software from Bruker AXS Inc. was used for Rietveld analysis.

The parameters for the crystal system, space group, and crystal structure of each mineral were assumed to be the same as those described in reference [17]. All amorphous substances were calculated by Eq. (22) from the quantitative value of the internal standard of Al_2O_3 [18].

$$A=\{100(S_R-S)/\{ S_R\,(100-S)/100\} \qquad \text{Eq. (22)}$$

where, A = proportion of amorphous substance (%), S = mixing rate of Al_2O_3 (%), S_R = quantitative value of Al_2O_3 (%)

Table 3 Chemical composition of cement and coefficients for particle size distribution

	ig.loss	Chemical Composition (%)								RR func.	
	(%)	SiO_2	Al_2O_3	Fe_2O_3	CaO	MgO	SO_3	Na_2O	K_2O	b	n
NC	2.4	20.2	5.39	3.04	64.6	0.92	1.91	0.30	0.31	0.035	1.15
LC	0.87	26.5	2.65	2.95	63.2	0.72	2.18	0.19	0.34	0.040	1.25

Table 4 Mineral composition of cement and other physical properties

	Density	Blaine	Composition by Bogue eq.				Rietveld analysis			
	(g/cm^3)	(cm^2/g)	C_3S	C_2S	C_3A	C_4AF	C_3S	C_2S	C_3A	C_4AF
NC	3.16	3300	63.3	10.3	9.1	9.2	58.6	17.2	7.0	9.9
LC	3.22	3430	27.3	55.5	2.0	9.0	30.6	54.6	0.8	8.2

Experimental results of degree of hydration of each constituents in NC and LC are presented in Fig. 2 and Fig. 3 respectively. In order to satisfy the experimental results, the parameters of CCBM are determined. The lists of parameter values are listed in Table 5.

From the experiment, the following results are obtained. In the higher temperature, namely curing temperature at 313K, the reaction of C_3A shows sign of leveling off at degree of hydration about 0.7, while in the case of C_4AF it is about 0.4. After sudden decrease in rate of hydration, they continuing very slow hydration. This phenomena can not be simulated by foregoing theoretical approach, the descriptive models shown as *2 and *3 in Table 5 are adopted to CCBM. Additionally the rate of hydration of C_2S has strong connectivity to the degree of hydration of

C_3S. This mutual relationship, which is shown in Fig. 4, is also modeled as phenomenal approach (*1 in Table. 5).

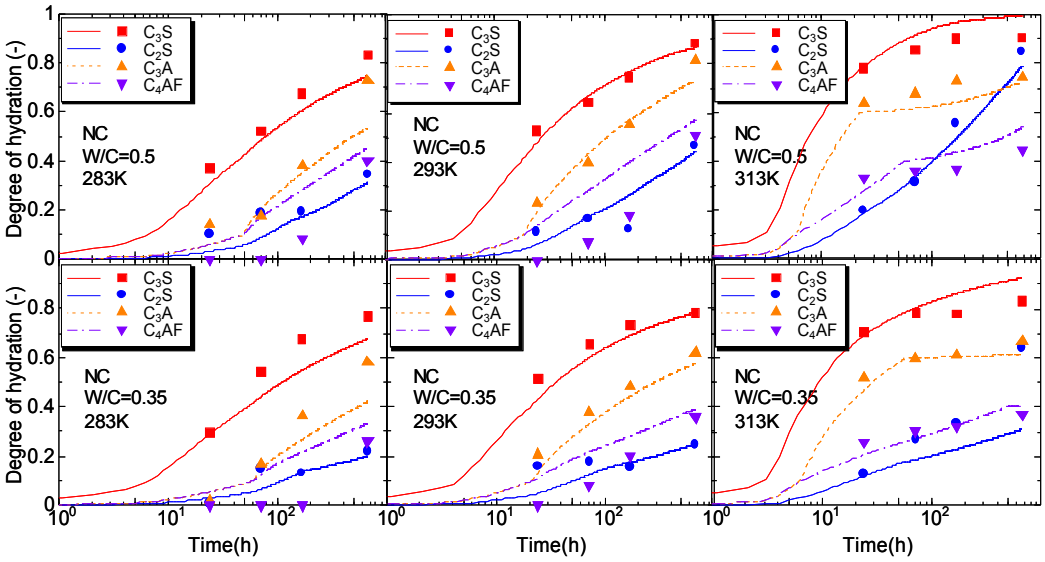

Fig. 2 Degree of hydration of C_3S, C_2S, C_3A and C_4AF in NC (marks) by Rietveld analysis and results of simulation by CCBM (lines).

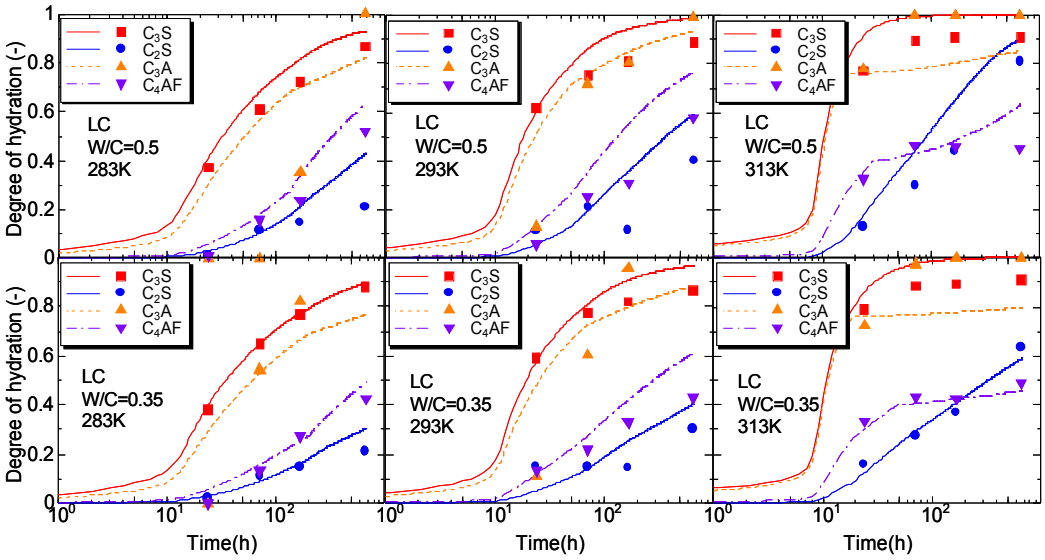

Fig. 3 Degree of hydration of C_3S, C_2S, C_3A and C_4AF in LC (marks) by Rietveld analysis and results of simulation by CCBM (lines).

4. Evaluation of model parameters

In order to evaluate the model parameters determined in former chapter, the experimental results for adiabatic temperature rise [6,19] are compared with those CCBM simulation. Getting the adiabatic temperature rise, heat capacity of concrete is assumed that it is equal to the summation of the heat capacity of each component; such as cement

hydrate (1.20 $Jg^{-1}K^{-1}$), unhydrated cement (0.78$Jg^{-1}K^{-1}$), water(4.19 $Jg^{-1}K^{-1}$), sand and aggregate(0.85 $Jg^{-1}K^{-1}$) [20].

The cement properties and mix proportions of concrete listed in Table 6. And the results of comparison are shown in Fig. 5. As is shown in Fig. 5, CCBM shows high potential for simulating the hydration process, even though the composition of cement is calculated by Bogue's equation. From these results, difference of predicted and experimental degree of hydration of each component shown in Fig. 2 and 3, as well as difference of initial ratio of each component predicted by XRD and Bogue's equation has rather minor effect on simulating adiabatic temperature curves within this limited case study.

Table 5 Values of model Parameters

	k_i (μm/h)	Ei/R (K)	
C_3S	0.07	6000	Eq.(8)
C_2S	0.004	3500	Eq.(9)
	C_{C2S}*k_{C2S}	3500	Eq.(9) *1
C_3A	0.01	7000	Eq.(10)
	0.03	7000	Eq.(11)
	0.001	7000	Eq.(11)*2
C_4AF	0.01	7000	Eq.(12)
	0.01	3000	Eq.(13)
	0.001	3000	Eq.(13)*3

*3: α_{C4AF}>0.4 and T>313K

Parameters	value	
B_{20} (μm/h)	0.01	Eq.(18)
b_1 (K)	1000	Eq.(18)
C (μm/h/mm^4)	10^{13}	Eq.(17)
$D_{e,20}$ (μm^2/h)	P_{C3S}x10^{-3} *4	Eq.(19)
b_2 (K)	15000	Eq.(19)

α_i : degree of hydration of each constituents
*1 : α_{C3S}>0.8 and C_{C2S}=1.5
*2 : α_{C3A}>0.7 and T>313K
*4: P_{C3S} is percentage of C_3S of cement

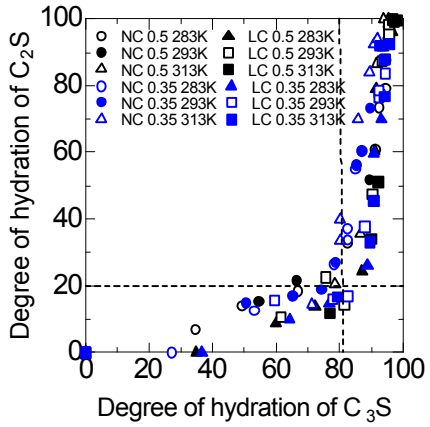

Fig. 4 Degree of hydration of C_2S as a function of that of C_3S

Table 6

	Composition by Bogue eq.					RR func.		Mix Proportion (kg/m^3)			
	C_3S	C_2S	C_3A	C_4AF	$C\bar{S}H_2$	b	n	W	C	S	G
OPC200	47	27	10	9	4	0.0303	1.1	157	200	862	1089
OPC400	47	27	10	9	4	0.0303	1.1	157	400	658	1129
LPC300	25	55	3	9	4	0.0263	1.2	145	300	811	1083

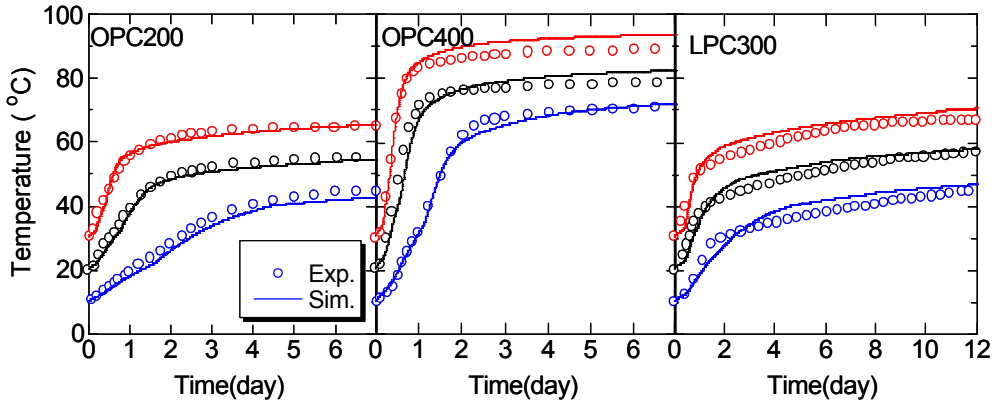

Fig. 5 Simulation of adiabatic temperature rise by CCBM compared with experimental results [6,19]

5. Conclusion

A numerical hydration model named CCBM, which take account of particle size distribution, inter-particle contact effect on rate of hydration, mineral composition of cement, and curing condition, is proposed. The parameters of the proposed model are determined from experimental data by Rietveld analysis. Potential of CCBM was evaluated through comparison of experimental and predicted adiabatic temperature curves on the condition that cement mineral composition was evaluated by Bogue's equation. Simulation results by CCBM showed good agreement with experimental data, which indicated that Bogue's equation is applicable for simulating adiabatic temperature curve with CCBM form the engineering point of view.

Acknowledgement

Conduction of XRD-Rietveld analysis was supported by Taiheiyo Cement Corporation.

References

[1] R. Kondo, S. Ueda, Kinetics and Mechanism of the Hydration of Cements, Fifth International Symposium on the Chemistry of Cements, Tokyo, (1968), II-4, pp.203-248

[2] F. Tomosawa, A Hydration model of cement, Proc. of Annual Meeting on Cement Technology, Cement Association of Japan, Vol.28, (1974), pp.53-57 (in Japanese)

[3] T. Knudsen, The Dispersion Model for Hydration of Portland Cement I., General Concepts, Cem Concr Res 14(5) (1984) 622-630

[4] H. M. Jennings and S. K. Johnson, Simulation of Microstructure Development During the Hydration of a Cement Compound, J Am Ceram Soc 69(11) (1986) 790-795

[5] K. van Breugel, Numerical Simulation of Hydration and Microstructural Development in Hardening Cement-Based Material (I) Theory and (II) Application, Cem Concr Res 25(2-3) (1995) 319-331 and 522-530

[6] T. Kishi and K. Maekawa, Thermal and mechanical modeling of yound concrete based hydration process of multi-component cement mirerals, in: R. Springerschmid (Ed.), Thermal Cracking in Concrete at early Ages, (1994), pp.10-18
[7] D. P. Bentz and E. J. Garboczi, Percolation of Phases in a Three-Dimensional Cement Paste Microstructural model, Cem Concr Res 21(2-3) (1991) 325-344
[8] F. Tomosawa, Development of a Kinetic Model for Hydration of Cement, Proceedings of 10th International Congress of Chemistry of Cement, (1997) pp.2ii051
[9] G. Frigione and S. Marra, Relationship between Particle Size Distribution and Compressive Strength in Portland Cement. Cem Concr Res 6 (1976) 113-128
[10] Y. Ono, Hydraulic Activity and Equilibrium Vapor Pressure of Clinker Compounds, JCA Proceedings of Cement & Concrete 44 (1990) 24-29
[11] D. A. Palmer, R. Fernandez-Prini, A. H. Harvey, Aqueous Systems at Elevated Temperatures and Pressures, Elsevier, London, 2004, pp. 1-29
[12] R. Badmann, N. Stockhausen, M. J. Setzer, The Statistical Thichness and the Chemical Potential of Adsorbed Water Films, J Col Int Sci 82(2) (1981) 534-542
[13] K. Uchida, Y. Fukubayashi, S. Yamashita, Effect of cement particle size on physical properties of cement paste, Proc. of Annual Meeting on Cement Technology, Cement Association Japan, 41 (1987) 62-65
[14] e.g. I. Odler, M. Rößler, Investigations on the relationship between porosity, structure and strength of hydrated Portland cement pastes. II. Effect of pore structure and of degree of hydration, Cem Con Res 15(3) (1985) 401-410
[15] D. Ménétrier, I. Jawed, T. S. Sun, J. Skalny, ESCA and SEM studies on early C_3S hydration, Cem Con Res 9(4) (1979) 473-482
[16] S. Hoshino, K. Yamada, H. Hirao, Analysis of hydration and strength development of cement containing blast furnace slag and limestone powder by using XRD/Rietveld method, Journal of Advanced Concrete Technology, 2006, (to be published)
[17] P. Stutzman, S. Leigh, NIST Technical Note 1441-Phase Composition Analysis of the NIST Reference Clinkers by Optical Microscopy and X-ray Powder Diffraction, 2002, pp.34-43
[18] R.C. Jones, C.J. Babcock, W.B. Knowlton, Estimation of the Total Amorphous Content of Hawaii Soils by Rietveld Method, Soil Science Society of America Journal, Vol64, 2000, pp.1100-1108
[19] Y. Otabe, Y Terano, Y. Suzuki, Properties of Temperature Rise of Belite Cement, JCA Proceedings of Cement & Concrete 51 (1997) 334-339
[20] I. Maruyama, T. Noguchi, T. Matsushita, Prediction of Adiabatic Temperature Rise in Portland Cement Concrete Using Computational Cement Based Material Model (in Japanese), Journal of structural and construction engineering (transactions of AIJ), 600 (2006) 1-8